Analytical Voltage Optimization Method for DC Railway Networks with Wayside Energy Storage System

Rojas Villarroel, J.A.; Bauer, P.; Rivera, S.

DOI
10.1109/IECON58223.2025.11221184

Publication date
2025

Document Version
Final published version

Published in
Proceedings of the IECON 2025 – 51st Annual Conference of the IEEE Industrial Electronics Society

Citation (APA)
Rojas Villarroel, J. A., Bauer, P., & Rivera, S. (2025). Analytical Voltage Optimization Method for DC Railway Networks with Wayside Energy Storage System. In *Proceedings of the IECON 2025 – 51st Annual Conference of the IEEE Industrial Electronics Society* (IECON Proceedings (Industrial Electronics Conference)). IEEE. https://doi.org/10.1109/IECON58223.2025.11221184

Analytical Voltage Optimization Method for DC Railway Networks with Wayside Energy Storage System

IECON 2025 – 51st Annual Conference of the IEEE Industrial Electronics Society | 979-8-3315-9681-1/25/$31.00 ©2025 EU | DOI: 10.1109/IECON58223.2025.11221184

1st Julian Rojas
Electrical Sustainable Energy department
Technische Universiteit Delft (TU Delft)
Delft, The Netherlands
J.A.RojasVillarroel@tudelft.nl

2nd Pavol Bauer
Electrical Sustainable Energy department
Technische Universiteit Delft (TU Delft)
Delft, The Netherlands
P.Bauer@tudelft.nl

3rd Sebastian Rivera
Electrical Sustainable Energy department
Technische Universiteit Delft (TU Delft)
Delft, The Netherlands
S.Rivera@tudelft.nl

***Abstract*—This study addresses a 1.8kV bilateral feeding system for DC railway applications, composed of multi-pulse diode rectifiers at both ends and a storage unit with a DC/DC converter located at an intermediate station. The storage system introduces an additional degree of freedom to control power flows by applying a specific voltage at a strategic point between the passive rectifiers. This paper formulates a voltage compensation problem aimed at reinforcing the network while minimizing conduction losses along the catenary. Due to the nonlinear nature of the power balance equations, a closed-form analytical solution is not directly obtained. To overcome this, the paper proposes an approximation method for the pantograph voltage to enable an analytical formulation of the optimization problem. A comparison between the proposed analytical approach and a numerical iterative optimization method is presented and discussed.**

***Index Terms*—Energy hub, energy storage, grid congestion, high power rectifiers, railways, traction.**

I. Introduction

TRANSPORTATION is a major contributor to greenhouse gas emissions and a key driver of climate change. In Europe, it accounts for approximately 20% of total greenhouse gas emissions, making the decarbonization of this sector a pressing priority. Among the various modes of transport, rail highlights as one of the most sustainable. Despite its relatively low carbon footprint, the railway sector is under increasing pressure to further reduce emissions in alignment with carbon neutrality targets set by industry stakeholders. These targets represent both an environmental necessity and an opportunity to displace fossil fuels as the dominant energy source in transport systems.

As urbanization accelerates and mobility demand increases, the load on distribution systems is expected to reach critical levels, especially with the rapid expansion of electric vehicle charging infrastructure and the broader electrification of transport. This trend will intensify existing challenges and may push distribution networks to their operational limits [1]–[5]. According to the European Commission, by 2030, all scheduled collective travel under 500 kilometers within the EU should be carbon neutral, and high-speed rail traffic is expected to double. These projections underscore the need for advanced and flexible energy strategies for the railway sector.

In this context, electric railway systems (ERS) must evolve alongside other rail-based transport modes such as trolleybuses and trams [6]–[8], leveraging new energy paradigms. One promising direction involves the integration of distributed energy resources (DERs), including renewable energy systems (RES) such as photovoltaic (PV) arrays and wind turbines, coupled with various forms of energy storage systems (ESSs). These combinations have demonstrated significant potential in enabling regenerative braking energy (RBE) recovery, improving energy efficiency, and supporting peak power shaving strategies [9]–[17]. Such services are especially critical in a 'Flex or Regret' scenario [18], where the increasing interdependency between the transport and energy sectors calls for proactive, adaptive planning to prevent infrastructure bottlenecks and avoid high-cost system overhauls. However, the implementation of these solutions often involves substantial infrastructure investments and technical complexities. To overcome these challenges effectively, it is essential to develop accurate mathematical models of railway power systems and to assess how sensitive system performance is to various modeling assumptions and parameter uncertainties. This paper contributes to this objective by presenting a sensitivity analysis of power demand profiles in DC railway systems, with particular focus on the implications for resistive power losses in the overhead catenary lines.

This study focuses on the Dutch DC railway traction power system (TPS), which is nominally rated at $1.5\,\mathrm{kV}$ and typically operated at $1.8\,\mathrm{kV}$. A representative layout of the system is shown in Fig. 1. The substations are based on multi-pulse diode rectifier for 12/24 pulse configuration. The train, on the other hand, will drain power from the catenary, divided between the two closest supply sources, although under heavy load conditions, the system may converge to a different solution. Despite its reliability and robustness over decades,

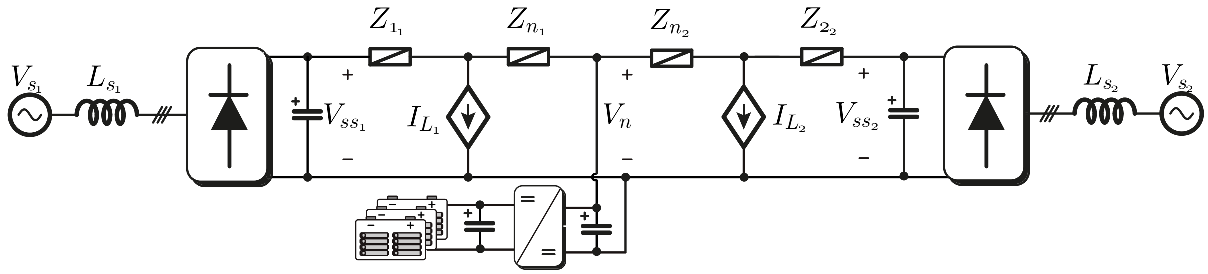

Fig. 1. DC railway power system electrical model.

it lacks controllability and struggles with current expansion plans. As the transportation sector undergoes electrification and decarbonization, the electricity demand is expected to increase. To address the some of above-mentioned challenges, current expansion plans are shifting toward localized energy generation and storage solutions. These decentralized approaches are not only more scalable and sustainable, but they also alleviate pressure on the national grid infrastructure expansion. In this context, power converters along with battery energy storage systems (BESS), renewable energy systems (RES) and advanced control strategies with advanced energy management methods offer a flexible and modular way to upgrade existing railway networks.

The proposed modernization strategy introduces an intermediate bidirectional DC/DC converter, connected to the catenary within a segment. Let's assume this conversion unit is properly designed and capable of regulating the voltage at the specified location while two trains are being fed. Given the limitations of the current TPS the converter output voltage will either reduce or increase the power coming into the segment from the two adjacent substations. Therefore, it is possible to fix the voltage in the intermediate segment of the railway to supply energy to the load, but also to set the system operation point where conduction losses are minimized. This problem involving conduction loss minimization through voltage control, has been previously explored in [19], where a coordinated control scheme between two controllable substations was proposed. In their work, the optimal substation voltages were determined using the Powell optimization method, effectively minimizing conduction losses along the catenary. Unlike their centralized approach, this paper investigates the use of a single controlled node placed at an intermediate location, aiming for similar benefits with potentially lower infrastructure complexity.

This paper is structured as follows. Section II introduces a problem formulation of power losses within a segment of the railway. Section III present an analytical approximation to provide a closed form to the optimization problem. Section IV presents the results of this approximation and some comparison in specific operation scenarios. Finally, a conclusion in provided in section V.

II. Problem Formulation

In Fig. 1 a bilaterally fed DC railway system with passive rectifier substations and an intermediate station equipped with a voltage-controlled DC/DC converter is presented for this study. In the current state of the system, the catenary losses are mainly given by the conditions of the loads. By adding a controllable voltage source in between both substations, it is possible to modify the power flow in the rail segment. This intermediate voltage acts as a degree of freedom to redistribute current flows among the substations, thus, the formulation of the problem aims to minimize the catenary losses across the section.

A. Catenary power losses

Assuming the substations at both ends are modeled as ideal voltage sources, the catenary conduction losses can be expressed as:

$$P_{\text{loss}} = \sum_{k\in\mathcal{L}} \left(\sum_{i\in\mathcal{S}} \frac{(V_i - V_{Lk})^2}{R_{ik}} + \frac{(V_n - V_{Lk})^2}{R_{nk}} \right) \tag{1}$$

$$\begin{aligned} P_{Lk} &= V_{L_k} \sum_{i\in\mathcal{S}} I_{ik} \\ I_{ik} &= \frac{V_i - V_{Lk}}{R_{ik}} \end{aligned} \tag{2}$$

Where I_{ik} is the current flowing from substation i into train k, V_i is the substation's i voltage, P_{Lk} is the DC power supplied to the train from the overhead line. On the other hand, $\mathcal{S}$ and $\mathcal{L}$ are the indexes associated with the supplying substations and the corresponding train. Note that if the system is perfectly balanced, the equation dictates that the power split among both substations only depends on the distance ratio between them. Therefore, the voltage at the train's pantograph from (3) has a quadratic solution in the form $0 = aV_{Lk}^2 + bV_{Lk} + c$, where the coefficients a, b, c depend on the substation voltages and the asymmetry in the circuit impedance. The parameters a, b, and c are defined as follows:

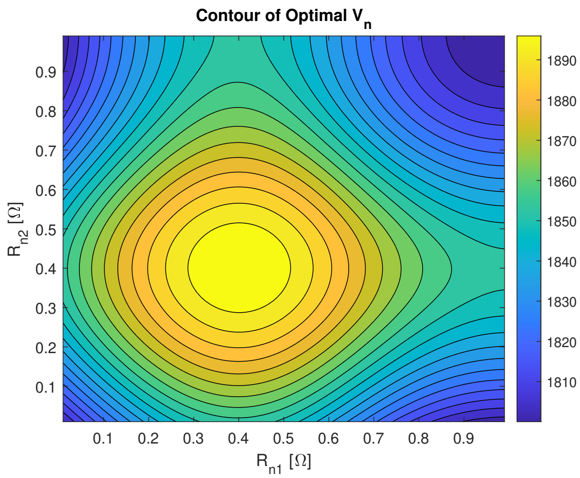

Fig. 2. Contour lines of optimal midpoint voltage V_n. Same case as in Fig. 3.

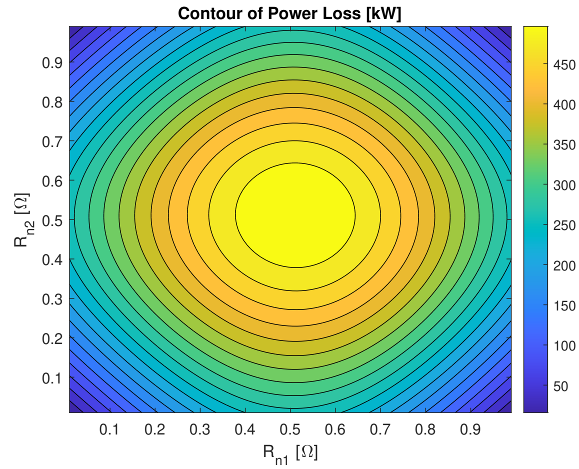

Fig. 3. Contour lines of total conduction losses as a function of V_n. Case: $P_{L1} = P_{L2} = 1.6\,\mathrm{MW}$, $V_1 = V_2 = 1800\,\mathrm{V}$.

$$a_k = \sum_{i=1}^{n} \frac{1}{R_i}$$
$$b_k = -\sum_{i=1}^{n} \frac{V_i}{R_i}$$
$$c_k = P_{Lk}$$

B. Derivation of an Optimal Power Flow

From equations (1) and (2), the total conduction losses depend quadratically on the voltage difference between the train location and the supply points. Using (2), the power delivered to the train P_{Lk} can be expressed as a nonlinear function of V_{Lk}:

$$P_{Lk} = V_{Lk} \sum_{i \in \mathcal{S}} \frac{V_i - V_{Lk}}{R_{ik}} = -a_k V_{Lk}^2 + b_k V_{Lk} \tag{3}$$

where the coefficients a_k and b_k are defined in (3). Solving this quadratic equation yields a unique and physically meaningful solution for V_{Lk}, provided that the discriminant $\Delta_k = b_k^2 - 4a_k P_{Lk}$ is non-negative.

Under traction conditions ($P_{Lk} > 0$) and assuming $V_i > V_{Lk}$, the resulting currents $I_{ik} > 0$, ensuring power flows from the substations into the train. However, since passive rectifiers at the adjacent substations do not support four-quadrant operation, the model assumes that energy during regenerative braking is absorbed exclusively by the energy storage system (ESS), and neglects interactions with other trains. This simplification could be relaxed by extending the model with logic-based rules for power exchange between trains and substations during regenerative events.

The expression in (3) motivates the formulation of an optimization problem in which the midpoint voltage V_n is calculated to minimize total conduction losses while satisfying power balance constraints at each train location:

$$\min_{V_n} \quad \sum_{k \in \mathcal{L}} \left(\sum_{i \in \mathcal{S}} \frac{(V_i - V_{Lk})^2}{R_{ik}} + \frac{(V_n - V_{Lk})^2}{R_{nk}} \right) \tag{4}$$

This results in a nested nonlinear optimization problem, where the total losses $P_{\text{loss}}(V_n)$ depend on the implicit function $V_{Lk}(V_n)$. Its gradient can be computed analytically as:

$$\frac{\partial P_{\text{loss}}}{\partial V_n} = \sum_{k \in \mathcal{L}} \left[\sum_{i \in \mathcal{S}} \frac{-2V_i + 2V_{Lk} \frac{\partial V_{Lk}}{\partial V_n}}{R_{ik}} + \frac{2V_n - 2V_{Lk} + 2V_{Lk} \frac{\partial V_{Lk}}{\partial V_n}}{R_{nk}} \right] \tag{5}$$

The sensitivity of V_{Lk} with respect to V_n is given by:

$$\frac{\partial V_{Lk}}{\partial V_n} = \frac{1}{2a_k R_{nk}} \left(1 - \frac{b_k}{\sqrt{\Delta_k}}\right) \tag{6}$$

$$V_{Lk} \frac{\partial V_{Lk}}{\partial V_n} = \frac{\sqrt{\Delta_k}}{4a_k^2 R_{nk}} \left(1 - \frac{b_k}{\sqrt{\Delta_k}}\right)^2 \tag{7}$$

Finally, the complete loss function becomes a nested mapping:

$$P_{\text{loss}}(V_n) = g\left(V_L(V_n), V_n\right) \tag{8}$$

Since $V_L(V_n)$ is not analytically expressible, the minimization of $P_{\text{loss}}(V_n)$ with respect to V_n becomes intractable analytically. The derivative:

requires applying the chain rule with an implicit derivative of V_L with respect to V_n, which involves a square root of a rational expression and again includes V_L. This structure leads to a non-closed-form gradient that must be computed numerically.

C. Optimization Problem Statement

Based on the analytical formulation described above, the voltage compensation strategy is posed as a nonlinear one-dimensional optimization problem:

$$\min_{V_n \in [V_{n,\min}, V_{n,\max}]} P_{\text{loss}}(V_n) \tag{9}$$

subject to:

- **Power balance constraint:** $P_{Lk} = V_{Lk}(V_n) \cdot I_{\text{total},k}(V_n) \quad \forall k \in \mathcal{L}$
- **Voltage bounds:** $V_{n,\min} \leq V_n \leq V_{n,\max}$, where $V_{n,\min} = 1600\,\text{V}$ and $V_{n,\max} = 1925\,\text{V}$

This problem is solved numerically using the `fminbnd` function in MATLAB, which implements a combination of golden-section search and parabolic interpolation for bounded univariate minimization. The total losses function $P_{\text{loss}}(V_n)$ is evaluated through nested expressions that capture the dependence of each train's voltage V_{Lk} on the midpoint voltage V_n, as described in (2) and (5).

The contour plots in Figures 3 and 2 illustrate the results of the numerical optimization for a representative case with two symmetric trains. In this example, the train power demands are set to $P_{L1} = P_{L2} = 1.6\,\text{MW}$, and both substations operate at $V_1 = V_2 = 1800\,\text{V}$. Figure 3 shows the resulting loss surface as a function of V_n, while Figure 2 presents the corresponding contour lines for the optimal midpoint voltage. Traction and electrical parameters were tailored according to the model presented in [20].

III. Analytical Approximation of Pantograph Voltage

To enable an analytical solution to the optimization problem, an explicit approximation of the pantograph voltage V_L as a function of the midpoint voltage V_n, train power demand P_{Lk}, substation voltage V_i, and the line resistance R_{nk} is proposed.

In order to keep the solution simple, it is important to perform a sensitivity analysis on the variables of the system. Clearly, all variables have a quadratic impact on the function V_{Lk}, the distance between the supply points being the most relevant, giving an intuition about using a paraboloid as an approximation function. However, according to 1, if the order of the polynomial function used to estimate V_{Lk} is greater than 1, the further algebraic expansion of the optimization function will also lead to a higher order polynomial solution which may need another numerical tool for solving it, or even worst, finding multiple minimal local solutions. Therefore, a simple function to characterize a linear relationship between V_n and V_{Lk}, while keeping a quadratic dependence on the variables V_i, R_{nk} and P_{Lk} is the following:

$$V_{Lk} \approx \alpha V_n + \beta P_{Lk}^2 + \gamma V_i^2 + \delta R_{nk}^2 \tag{10}$$

The coefficients $\alpha, \beta, \gamma, \delta$ are derived by a regression process based on numerical evaluations of the exact model. This function structure ensures that the key nonlinear dependencies of V_L are captured within a certain range, while maintaining a structure that allows algebraic manipulation. It is important to mention that the proposed structure is fitted using the closest region of the paraboloid ($R_{n1}, R_{n2} \leq 0.15$. where the impact on the load is critical since the train could be accelerating while the distance between any supply point and the train is acceptable. The main reason for this assumption is to give special focus under heavy load scenarios.

The approximation reflects the dependencies observed in the equations presented in the previous section. This structure allows to obtain an analytical solution for the minimum total loss function for $\hat{V}_n^*$.

A. Closed-Form Expression for Losses

Using the approximation for the pantograph voltage V_{Lk} introduced in (10), we substitute it into the total loss expression given in (1). For each train $k \in \mathcal{L}$, the contribution to the total losses becomes:

$$P_{\text{loss},k} = \sum_{i \in \mathcal{S}} \frac{(V_i - V_{Lk})^2}{R_{ik}} + \frac{(V_n - V_{Lk})^2}{R_{nk}} \tag{11}$$

Substituting $V_{Lk} \approx \alpha V_n + \beta P_{Lk}^2 + \gamma V_i^2 + \delta R_{nk}^2$ into the expression above yields a quadratic function of V_n, given that all other terms are treated as constants with respect to V_n. This results in a total loss function of the form:

$$P_{\text{loss}}(V_n) = aV_n^2 + bV_n + c \tag{12}$$

where the coefficients a, b, c are computed by grouping terms after substitution and simplifying:

$$a = \sum_{k \in \mathcal{L}} \left(\sum_{i \in \mathcal{S}} \frac{\alpha^2}{R_{ik}} + \frac{(1-\alpha)^2}{R_{nk}} \right), \tag{13}$$

$$b = \sum_{k \in \mathcal{L}} \left(\sum_{i \in \mathcal{S}} \frac{-2\alpha(V_i - C_k)}{R_{ik}} - \frac{2(1-\alpha)C_k}{R_{nk}} \right), \tag{14}$$

$$c = \sum_{k \in \mathcal{L}} \left(\sum_{i \in \mathcal{S}} \frac{(V_i - C_k)^2}{R_{ik}} + \frac{C_k^2}{R_{nk}} \right). \tag{15}$$

where $C_k = \beta P_{Lk}^2 + \gamma V_i^2 + \delta R_{nk}^2$.

The optimal midpoint voltage minimizing this quadratic loss function is then obtained in closed form as:

$$\hat{V}_n^* = -\frac{b}{2a} \tag{16}$$

This result provides a fast and interpretable way to estimate the optimal voltage setpoint for the DC/DC converter under different loading conditions and train locations.

IV. Results and Discussions

To evaluate the accuracy of the proposed analytical approximation, we compare its results with those obtained using the numerical optimization method `fminbnd` in MATLAB. Two scenarios are considered:

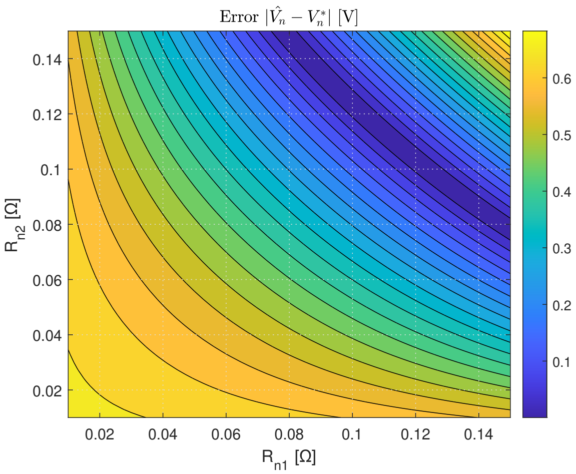

Fig. 4. Absolute error between analytical and numerical V_n under balanced scenario. $V_1 = V_2 = 1800[V]$, $P_{L1} = P_{L2} = 1.5[MW]$.

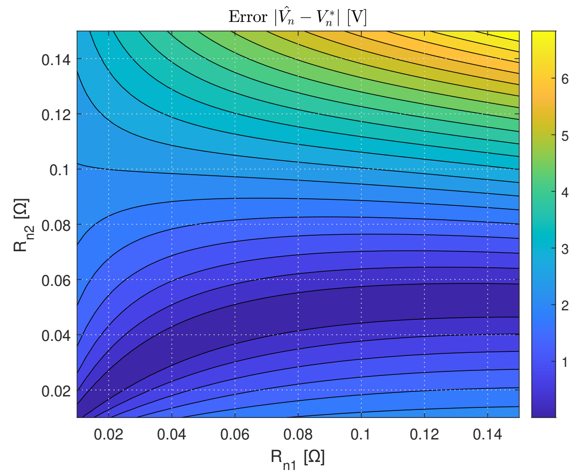

Fig. 5. Absolute error between analytical and numerical V_n under unbalanced scenario. $P_{L1} = 1.5$MW, $P_{L2} = 2.0$ MW and $V_1 = 1750$V, $V_2 = 1700$ V.

- **Balanced scenario:** Identical power demands and symmetric positions for both trains, with $P_{L1} = P_{L2} = 1.5$ MW and $V_1 = V_2 = 1800$ V.
- **Unbalanced scenario:** One train is under higher load, and the distances to substations are asymmetric. $P_{L1} = 1.5$MW, $P_{L2} = 2.0$ MW and $V_1 = 1750$V, $V_2 = 1700$ V.

Figure 4 shows the absolute error between the analytical and numerical solutions for V_n in the balanced case. The maximum error observed is 0.65V, which is negligible in the context of 1.6kV–1.8kV voltage levels. In the unbalanced scenario (Figure 5), the maximum absolute error increases to 6.6V due to the larger nonlinearities introduced by the overloading condition and asymmetric supply resistances.

In both cases, there are regions where the error approaches zero, indicating that the analytical approximation successfully captures the key nonlinear behavior of the system within the region of interest ($0.05 < R_{nk} < 0.15$). This validates the use of the closed-form expression in scenarios where fast, real-time estimation is required, such as on-board converters or decentralized control schemes.

The analytical model significantly reduces computational complexity and enables insights into the behavior of the system, particularly under normal operation conditions. The error remains bounded and small in practical cases, suggesting that the model is not only computationally efficient but also robust within the selected operating range.

Tables I and II summarize the approximation errors across four scenarios, for two different ranges of normalized resistance values: $R_{nk} \leq 0.35$ and $R_{nk} \leq 0.35$. These ranges reflect practical limits for DC railway line impedance, where smaller values are typical under nominal loading and cable configurations, while higher values can occur under degraded conditions or long distances.

Within the range ($R_{nk} \leq 0.15\Omega$), shown in Table I, the analytical approximation performs very well, with root mean square errors (RMSE) below 4.3V in all scenarios. Notably, Scenario 1—representing nearly balanced load and resistance conditions—achieves a maximum error below 1V and an average error under 0.4V, highlighting the high accuracy of the model under ideal or nominal configurations. Scenario 4 also shows excellent performance, with errors similar to Scenario 1 despite some asymmetry.

For higher loading differences or asymmetric resistances, the RMSE increases slightly, reaching up to 4.28V in Scenario 3. However, these errors are still acceptable for real-time voltage estimation purposes, especially considering the voltage scale of operation (typically 1600–1925V).

To include higher resistances ($R_{nk} \leq 0.35\Omega$), as shown in Table II, the approximation error increases significantly. In this extended range, RMSEs range from 3.5V to 16.7V, and maximum errors can exceed 50V (Scenario 3). This degradation is expected due to the stronger nonlinear effects introduced at higher resistances, where the underlying assumptions of the quadratic loss model become less accurate. Despite this, the model still preserves qualitative trends and could be used for estimation with caution under such conditions.

Overall, these results confirm that the proposed closed-form approximation is especially well-suited for normal operating conditions (i.e., $R_{nk} \leq 0.15\Omega$), where it delivers low error and fast computation. This makes it particularly attractive for real-time control or embedded applications. For broader operation ranges, adaptive models or piecewise approximations could be explored in future work to maintain accuracy.

TABLE I
ERROR BETWEEN $\hat{V}_n$ AND V_n^* FOR DIFFERENT SCENARIOS FOR $R_{nk} \leq 0.15$

Scenario	**RMSE [V]**	**Max [V]**	**Min [V]**	**Mean [V]**
Scenario 1	0.4336	0.7167	0.0002	0.3906
Scenario 2	2.2035	3.7345	1.0604	2.1353
Scenario 3	4.2792	8.2526	2.5682	4.1047
Scenario 4	2.6564	6.0503	0.0002	2.4059

TABLE II
ERROR BETWEEN $\hat{V}_n$ AND V_n^* FOR DIFFERENT SCENARIOS FOR $R_{nk} \leq 0.35$

Scenario	RMSE [V]	Max [V]	Min [V]	Mean [V]
Scenario 1	3.5082	12.965	0.0020	2.3485
Scenario 2	7.0014	21.027	1.0604	5.7550
Scenario 3	16.701	51.050	2.5686	13.222
Scenario 4	13.628	43.639	0.0040	10.333

V. CONCLUSION

This work presented an analytical approximation for estimating the optimal midpoint voltage V_n in DC railway systems with passive substations and resistive line losses. The proposed model is based on a closed-form approximation of the train terminal voltage V_L, expressed as a quadratic function of system parameters around typical operating points. This expression was then used to derive an approximate loss function, enabling direct minimization without iterative numerical optimization.

A detailed comparison with the reference numerical solution, obtained via `fminbnd`, demonstrates that the analytical model achieves good accuracy within the typical operating range ($R_{nk} \leq 0.15\Omega$). In this domain, the root mean square error remains below 5V in all tested scenarios, and often below 1V under balanced conditions. Even when extended to higher resistance values ($R_{nk} \leq 0.35\Omega$), the model preserves qualitative accuracy, though with increased error due to stronger nonlinear effects.

The simplicity and low computational cost of the proposed approximation make it particularly suitable for embedded control, real-time optimization, and on-board power management in DC railway systems. Future work may address extending the model to dynamic scenarios with time-varying loads and include adaptive corrections or hybrid methods to maintain accuracy under broader operating conditions. For instance, considering that the train usually accelerates during the first phase, it could be acceptable to assume the train operates at constant power demand while coasting (larger resistance, low power), potentially reducing the non linear dependence within the variables.

ACKNOWLEDGMENT

The authors would like to thank the Europe's Rail program, Nederlandse Spoorwegen (NS) and ProRail working together to research feasible solutions for enhance the DC power system. This study is part of work package 11.1 of Rail4Earth, where similar pilots are built addressing different environments. The FP4 - Rail4EARTH project under Grant Agreement n°101101917 is supported by the Europe's Rail Joint Undertaking and its members.

REFERENCES

[1] A. Ipakchi and F. Albuyeh, "Grid of the future," *IEEE power and energy magazine*, vol. 7, no. 2, pp. 52–62, 2009.

[2] K. J. Dyke, N. Schofield, and M. Barnes, "The impact of transport electrification on electrical networks," *IEEE Transactions on Industrial Electronics*, vol. 57, no. 12, pp. 3917–3926, 2010.

[3] S. Rivera, S. M. Goetz, S. Kouro, P. W. Lehn, M. Pathmanathan, P. Bauer, and R. A. Mastromauro, "Charging infrastructure and grid integration for electromobility," *Proceedings of the IEEE*, 2022.

[4] S. Khayyam, F. Ponci, J. Goikoetxea, V. Recagno, V. Bagliano, and A. Monti, "Railway energy management system: Centralized–decentralized automation architecture," *IEEE Transactions on Smart Grid*, vol. 7, no. 2, pp. 1164–1175, 2015.

[5] M. Botte, L. D'Acierno, and M. Pagano, "Impact of railway energy efficiency on the primary distribution power grid," *IEEE Transactions on Vehicular Technology*, vol. 69, no. 12, pp. 14 131–14 140, 2020.

[6] I. Diab, G. R. C. Mouli, and P. Bauer, "A review of the key technical and non-technical challenges for sustainable transportation electrification: A case for urban catenary buses," in *2022 IEEE 20th International Power Electronics and Motion Control Conference (PEMC)*. IEEE, 2022, pp. 439–448.

[7] I. Diab, A. Saffirio, G. R. C. Mouli, A. S. Tomar, and P. Bauer, "A complete dc trolleybus grid model with bilateral connections, feeder cables, and bus auxiliaries," *IEEE Transactions on Intelligent Transportation Systems*, vol. 23, no. 10, pp. 19 030–19 041, 2022.

[8] T. Kamel, M. Zangiabadi, H. Dong, Z. Tian, N. Wade, V. Pickert, and P. Tricoli, "Practical demonstration and novel optimization control for a smart soft open point to maximize the synergy between the dc metro line and the lv distribution grid," *IEEE Transactions on Transportation Electrification*, vol. 11, no. 1, pp. 1298–1312, 2024.

[9] J. A. Aguado, A. J. S. Racero, and S. de la Torre, "Optimal operation of electric railways with renewable energy and electric storage systems," *IEEE Transactions on Smart Grid*, vol. 9, no. 2, pp. 993–1001, 2016.

[10] J. Pouget, B. Guo, L. Bossoney, J. Coppex, D. Roggo, and C. Ellert, "Energetic simulation of dc railway micro-grid interconnecting with pv solar panels, ev charger infrastructures and electrical railway network," in *2020 IEEE Vehicle Power and Propulsion Conference (VPPC)*. IEEE, 2020, pp. 1–7.

[11] Y. Ge, H. Hu, J. Chen, K. Wang, and Z. He, "Combined active and reactive power flow control strategy for flexible railway traction substation integrated with ess and pv," *IEEE Transactions on Sustainable Energy*, vol. 13, no. 4, pp. 1969–1981, 2022.

[12] M. Brenna, F. Foiadelli, and H. J. Kaleybar, "The evolution of railway power supply systems toward smart microgrids: The concept of the energy hub and integration of distributed energy resources," *IEEE Electrification Magazine*, vol. 8, no. 1, pp. 12–23, 2020.

[13] E. P. de la Fuente, S. K. Mazumder, and I. G. Franco, "Railway electrical smart grids: An introduction to next-generation railway power systems and their operation." *IEEE Electrification Magazine*, vol. 2, no. 3, pp. 49–55, 2014.

[14] P. Yao, H. Wang, Y. Liu, J. Niu, Z. Zhu, and L. Lin, "Integrated railway smart grid architecture based on energy routers," *Chinese Journal of Electrical Engineering*, vol. 7, no. 4, pp. 93–106, 2021.

[15] J. Lin, S. Hu, Y. Li, J. Zhang, J. Zhang, and J. Yu, "A framework-compatible hierarchical railway power regulation strategy with the integration of energy storage-embedded railway power flow controller," *IEEE Transactions on Transportation Electrification*, vol. 10, no. 3, pp. 7297–7309, 2023.

[16] D. Choi, J.-H. Park, and J.-S. Lee, "Individual module power control of solid-state transformer for multiport configuration in railway traction systems," *IEEE Transactions on Transportation Electrification*, 2024.

[17] J. Chen, H. Hu, M. Wang, Y. Ge, K. Wang, Y. Huang, K. Yang, Z. He, Z. Xu, and Y. R. Li, "Power flow control-based regenerative braking energy utilization in ac electrified railways: Review and future trends," *IEEE Transactions on Intelligent Transportation Systems*, vol. 25, no. 7, pp. 6345–6365, 2024.

[18] E. Beckstedde and L. Meeus, "From "fit and forget" to "flex or regret" in distribution grids: dealing with congestion in european distribution grids," *IEEE power and energy magazine*, vol. 21, no. 4, pp. 45–52, 2023.

[19] D. González and F. Manzanedo, "Power losses minimization in dc electric railways by means of traction substations coordinated voltage control," in *IET Conference on Railway Traction Systems (RTS 2010)*. IET, 2010, pp. 1–5.

[20] J. Rojas, S. Rivera, I. Diab, and P. Bauer, "A sensitivity analysis for power profile modeling: A case study of dutch dc railway networks," in *2024 International Symposium on Power Electronics, Electrical Drives, Automation and Motion (SPEEDAM)*. IEEE, 2024, pp. 1081–1086.